Lab on a Chip

Accepted Manuscript

This is an *Accepted Manuscript*, which has been through the Royal Society of Chemistry peer review process and has been accepted for publication.

Accepted Manuscripts are published online shortly after acceptance, before technical editing, formatting and proof reading. Using this free service, authors can make their results available to the community, in citable form, before we publish the edited article. We will replace this *Accepted Manuscript* with the edited and formatted *Advance Article* as soon as it is available.

You can find more information about *Accepted Manuscripts* in the Information for Authors.

Please note that technical editing may introduce minor changes to the text and/or graphics, which may alter content. The journal's standard Terms & Conditions and the Ethical guidelines still apply. In no event shall the Royal Society of Chemistry be held responsible for any errors or omissions in this *Accepted Manuscript* or any consequences arising from the use of any information it contains.

ROYAL SOCIETY OF CHEMISTRY

www.rsc.org/loc

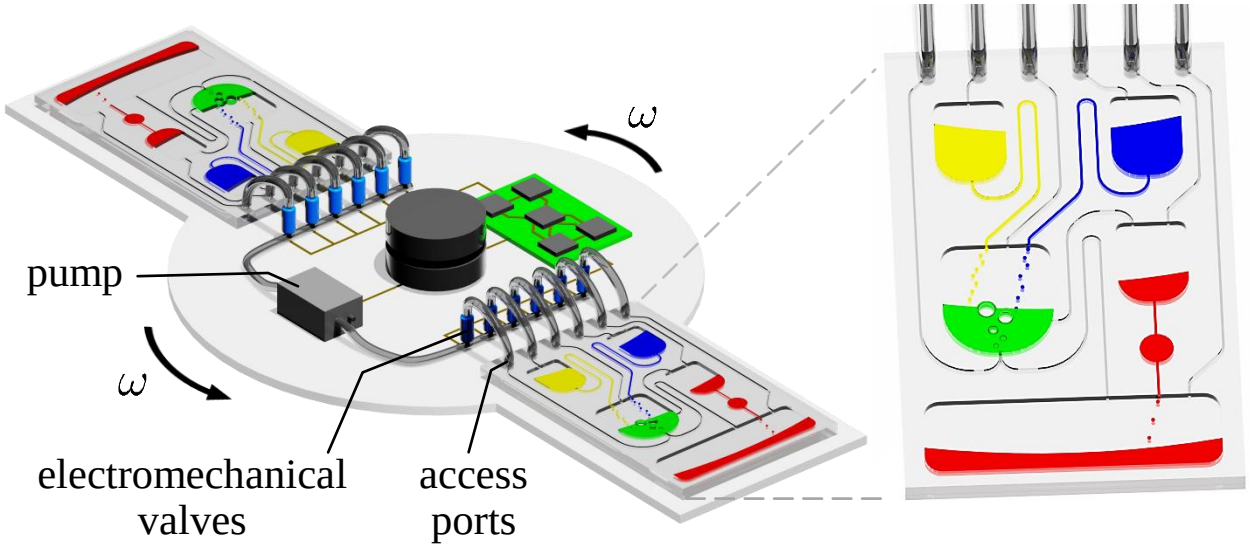

Active pneumatic pumping of liquids on lab-on-a-chip platforms by combining centrifugal fields and electromechanically controlled external pressure.

Lab on a Chip Accepted Manuscript

Journal Name

Dynamic Article Links ►

Cite this: DOI: 10.1039/c0xx00000x

www.rsc.org/xxxxxx

ARTICLE TYPE

Active pneumatic control of centrifugal microfluidic flows for lab-on-a-chip applications

Liviu Clime‡, Daniel Brassard‡, Matthias Geissler and Teodor Veres*

Received (in XXX, XXX) Xth XXXXXXXXX 20XX, Accepted Xth XXXXXXXXX 20XX
DOI: 10.1039/b000000x

This paper reports a novel method of controlling liquid motion on a centrifugal microfluidic platform based on the integration of a regulated pressure pump and a programmable electromechanical valving system. We demonstrate accurate control over the displacement of liquids within the system by pressurizing simultaneously multiple ports of the microfluidic device while the platform is rotating at high speed. Compared to classical centrifugal microfluidic platforms where liquids are solely driven by centrifugal and capillary forces, the method presented herein adds a new degree of freedom for fluidic manipulation, which represents a paradigm change in centrifugal microfluidics. We first demonstrate how various core microfluidic functions such as valving, switching, and reverse pumping (i.e., against the centrifugal field) can be easily achieved by programming the pressures applied at dedicated access ports of the microfluidic device. We then show, for the first time, that the combination of centrifugal force and active pneumatic pumping offers the possibility of mixing fluids rapidly (~0.1 s) and efficiently based on the creation of air bubbles at the bottom of a microfluidic reservoir. Finally, the suitability of the developed platform for performing complex bioanalytical assays in an automated fashion is demonstrated in a DNA harvesting experiment where recovery rates of about 70% were systematically achieved. The proposed concept offers the interesting prospect to decouple basic microfluidic functions from specific material properties, channels dimensions and fabrication tolerances, surface treatments, or on-chip active components, thus promoting integration of complex assays on simple and low-cost microfluidic cartridges.

Lab on a Chip Accepted Manuscript

Cite this: DOI: 10.1039/c0xx00000x

www.rsc.org/xxxxxx

ARTICLE TYPE

1 Introduction

Centrifugal microfluidics uses centrifugal forces on rotating platforms to manipulate and control liquids.[1-3] Centrifugal systems are appealing for developing sample-to-answer platforms for biomedical and diagnostic applications[4, 5] where they have been shown, for example, to effectively support cell-based assays,[6, 7] sample lysis,[8, 9] nucleic acid amplification using polymerase chain reaction (PCR),[10, 11] DNA microarray hybridization[12, 13] and single-molecule detection.[14]

Most centrifugal microfluidic systems rely on capillary[1, 15] and siphon[16] valves to control the passage of fluid both temporally and spatially. The main drawback of these flow control units is that their functioning and performance depend on the wetting properties of the materials used in the fabrication process, which can show variation and instability over time and often require complex surface treatments before assembly of the devices. Moreover, capillary valves can be effective for a narrow range of liquid-solid contact angles only[1, 17] and they are prone to untimely priming or blocking due to variability in the contact angle hysteresis, the quality of the microchannels and corner segments[18] associated with the fabrication techniques.

Various strategies have been developed in an attempt to solve these issues. For example, wax plugs have been integrated in centrifugal microfluidic devices to block liquids until heat is applied.[19, 20] Similarly, valves or pumps based on dissolvable films[21, 22] or magnetic forces[23] have also been demonstrated recently. While effective, the implementation of such active components on a chip increases substantially the fabrication complexity of the devices. For example, the integration of dissolvable films requires the alignment and bonding of 8 different polymer layers.[22] Complex fabrication schemes are typically associated with high cost which is detrimental to biomedical and analytical applications where work flow and regulatory requirements necessitate the development of single-use, low-cost microfluidic devices.

There have been various attempts to use pneumatic forces generated inside sealed chambers to create or improve certain microfluidic functions. For example, pneumatic energy can be stored temporarily on-chip by compressing air pockets[24, 25] or deforming a flexible membrane[26, 27] using the centrifugal force generated by a liquid at high rotational speeds. Alternatively, pneumatic forces can be generated by heating or cooling the air trapped in closed (non-vented) chambers.[26, 28] Finally, microfluidic control elements coined as centrifugo-pneumatic valves[25] have been proposed to facilitate metering of highly wetting liquids.

While some simple fluidic functions have been already demonstrated with these approaches, they typically offer relatively limited additional control over the fluid manipulation. Also, the proposed actuation mechanisms based on heating are relatively slow and may interfere with biological assays (involving sensitive enzymes, for example) requiring precise control of the temperature. Finally, the integration of large chambers to store pneumatic energy increases the total footprint for a given protocol, diminishing drastically the number of operations that can be performed in a single run.

Another proposed method to manipulate liquids in centrifugal microfluidics consists of blowing compressed air on the surface of rotating microfluidic devices using a nozzle that is connected to a fixed (non-rotating) external reservoir.[29-31] The liquid placed inside the device can then experience a force pulse each time the access port is passing through the stream. While various fluidic functions have been achieved with this approach, the intrinsically intermittent nature of the actuation leads to several limitations. For example, it limits the possibility to address multiple access ports simultaneously and prevents the application of a controlled regulated pressure to the device. Also, the number of possible independent air injection sites is limited since the air jet is applied on the entire circumference of the device during rotation. Finally, the use of an external air jet induces the risk of expelling liquid out of an access hole,[31] which cannot be tolerated for applications where harmful reagents or pathogenic samples are processed.

In summary, despite of the various innovative approaches attempted to facilitate the manipulation of fluids, a straightforward solution for reliable and cost-effective integration of complex bioanalytical assays in centrifugal microfluidics is still lacking. Here, we propose a novel concept that we coin active pneumatic pumping in centrifugal microfluidics. This concept relies on the accurate control of the air pressure at dedicated access ports of the microfluidic device by embedding, on the rotating platform, a regulated pump, miniature electro-mechanical valves and a programmable microcontroller. We first describe the proposed concept and review the advantages provided by the new approach. We then present microchip designs accompanied by experimental demonstrations for the implementation of several basic microfluidic functions including valving, switching and reverse pumping. Moreover, we propose a novel and highly efficient method of agitating and mixing multiple liquid components in a microchamber using generation and rising of air bubbles against the centrifugal force field. We finally present an on-chip DNA harvesting experiment to demonstrate how active pneumatic pumping facilitates integration of bioanalytical assays using centrifugal microfluidics.

2 Active pneumatic pumping in centrifugal microfluidics

The most important difficulty in centrifugal microfluidics is to displace liquids from one chamber to another in a controlled and reproducible manner. The implementation of vents (i.e., access ports opened to atmospheric pressure p_{atm}) is central for liquids to both empty and fill those reservoirs. Without the presence of a

Lab on a Chip Accepted Manuscript

Cite this: DOI: 10.1039/c0xx00000x

www.rsc.org/xxxxxx

ARTICLE TYPE

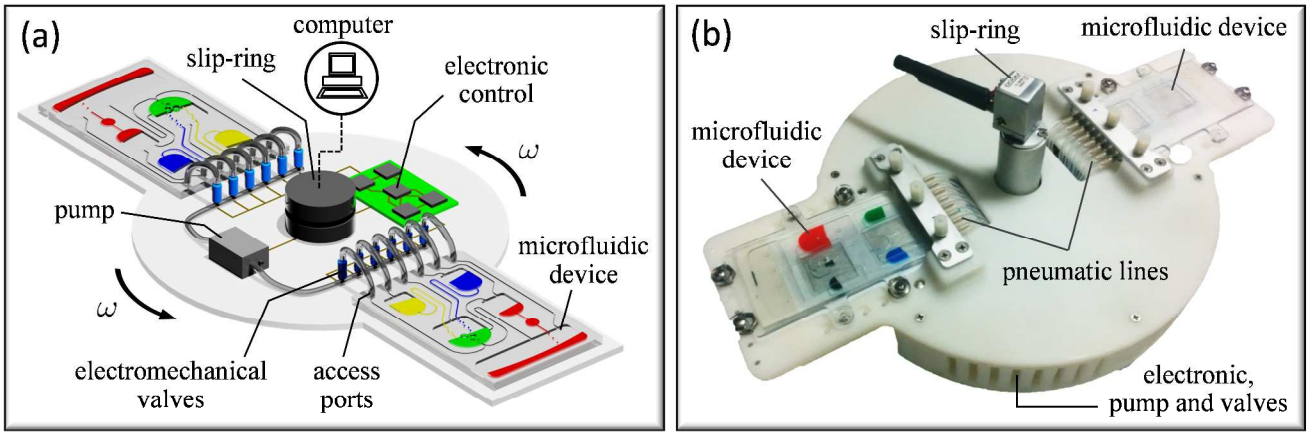

Fig. 1 Implementation of active pneumatic pumping on a centrifugal microfluidic platform. (a) Schematic depicting the arrangement of the different components in the system. (b) Photograph of the microfluidic platform as it was used within this work. See text for details.

vent, air trapped inside cavities would eventually impede or even stop liquid displacement by compensating for the pressure difference induced by the centrifugal field. In the more general manner, if a liquid plug is connected to two ports of pressures p_1 and p_2 then the equation for the steady state flow in a centrifugal force field can be written as (neglecting capillary forces)

$$p_1 - p_2 + \frac{1}{2}\rho\omega^2(r_2^2 - r_1^2) = R_{hyd}Q \qquad (1)$$

where ρ is the density of the liquid, ω is the angular velocity of the spinning platform, r_1 and r_2 the positions of receeding and advancing menisci, respectively, R_{hyd} the hydraulic resistance of the fluidic path and Q the flow rate of the liquid. In classical centrifugal microfluidics, the two ports work in fact as regular vents since they are always connected to open air such that $p_1 = p_2 = p_{atm}$ and the above equation reduces to the centrifugal pressure and the hydraulic terms only. As a consequence, both terms in this equation are positive and the liquid always flows from the centre toward the rim of the centrifugal disk ($Q \geq 0$). This induces serious limitations to the number of microfluidic operations that can be implemented due to the finite length of the microfluidic chip. From an application point-of-view, this well-known "footprint problem" can be highly problematic as it means that only a relatively low number of operations can be performed on a given microfluidic device. The problem could be alleviated if liquids could be pumped back to the centre allowing for the implementation of multi-step processes while making efficient use of the disk space. Achieving good control over the pressures $p_1$and p_2 is thus a key factor for improving the control over liquid flow and displacement.

In an attempt to reverse the direction of the flow ($Q < 0$) Thio *et al.*[26] connected the vent p_2 to an air chamber heated by infra-red irradiation. In this way, the pressure p_2 is controlled by the temperature of the air in this chamber. Alternatively, the same function has been implemented by Aeinehvand *et al.*[27] using latex micro-balloons as compression chambers to store the energy from the centrifugal field and release it at will by lowering the rotation speed. Also, as discussed previously, Kong and Salin[29-31] simply blow air to an access port using a compressed air reservoir to momentarily increase the pressure in the respective chamber. However, as discussed before, these approaches are hardly practical for most part of biological applications mainly due to the limitations related to the accurate control of the pressure and the distribution of the actuation ports.

Building on these developments, we extended the control of the pressure in a microfluidic device by connecting the vents of the fluidic chambers to a number of dedicated ports actuated by an external pressure pump through a set of electromechanical valves that are mounted on the rotating centrifugal platform (Fig. 1a). The pump and the electromechanical valves are controlled with the help of a microcontroller connected to a computer either wirelessly or by using a slip-ring, thus enabling direct real-time programming of the pneumatic pressure while the platform is rotating at high speed.

The elements required for controlling the pneumatic pressure can be integrated in different configurations on the centrifugal platform. For example, three-way electromechanical valves can be used to connect the access ports to either atmospheric pressure or to the pressure generated by the pump. The pump could also be reversed in order to provide a pressure either higher or lower than atmospheric pressure adding in this way a new degree of freedom to the fluidic manipulation. It may equally be feasible to obtain pressure from one or more pressurized containers (potentially containing various types of gases or liquids) or by using pneumatic slip-rings. Alternatively, two-way electro-mechanical valves can be used to directly block or open the access ports of the devices. In this way, it becomes possible to create interesting fluidic functions, by simply restructuring in real-time which

Lab on a Chip Accepted Manuscript

chambers of the microfluidic devices are vented and which are blocked without even using a pressure pump at all. For example, the electrical power required to operate the valves, the pump, and the microcontroller can be transferred through a slip-ring, electromagnetic induction elements or can be directly integrated on the platform using batteries. Of course, once the active pneumatic components are in place, it becomes straightforward to integrate various other electrical control elements on the platform, including pressure sensors, pressure regulators, heating elements, temperature sensors, electrochemical sensors, and optical or fluorescence detectors, among others.

Figure 1b shows an example of an active pneumatic centrifugal microfluidic platform that we have developed and used in the present work. This platform contains 8 independent active pneumatic lines that can be connected either to atmospheric pressure or to the pressure generated by an on-board pump (adjustable in real-time in the range of 0 to 5 psi above p_{atm}; see Section 3.1 for details). A simple standardized pressure manifold is used to connect the pneumatic lines to the access ports of the microfluidic devices. This platform can accommodate two identical microfluidic devices connected to the same pneumatic system. As a result, the two devices receive the same pressure dose, providing the possibility to perform two identical assays at the same time. To perform more than two assays in parallel, the pneumatic lines would have to be split further on accordingly. The developed platform also contains all the electronics required to rapidly control and monitor the temperature on four independent zones (i.e., two zones per device). All the electronic components, valves, pump, sensors and tubing are integrated on a bottom plate placed inside the centrifugal platform (not visible in Fig. 1b). The system is enclosed with a hard cover plate that supports the microfluidic devices. The platform is controlled in real-time with an in-house computer software that gives access to different microcontrollers responsible for the temperature control, pump pressure, electromechanical valves and rotation speed.

We believe that the integration of active pneumatic pumping in centrifugal microfluidics offers several advantages compared to previous approaches. By connecting the access ports directly to a pressure manifold we not only eliminate the risk of liquid splashing and associated contamination from the air jet pumping approach[29-31] but also enable application of controlled pressure on multiple ports simultaneously. Precise, reproducible and controlled liquid displacements can therefore be obtained in a completely sealed system. Also, we avoid the high complexity induced by additional chambers,[26, 28] long capillary channels[16] or elastomeric[27] and magnetic[32] materials integrated on the chip. Compared to classical centrifugal microfluidics, the only additional step required by the proposed approach consists of connecting access ports of the device with a standard manifold, which can however easily be integrated in the chip-holding mechanism (as implemented in the platform shown in Fig. 1b).

The proposed approach also brings several advantages for the design and fabrication of microfluidic devices. Microfluidic functions become independent of the dimensions of the communicating channels and related features at the chip level. They are rather controlled solely by varying the two parameters p_1 and p_2 in Eq. (1). Consequently, large scale fabrication processes including injection moulding, thermoforming or roll-to-roll hot-embossing can be envisaged. The choice of materials also increases since fluid behaviour does not rely on capillarity and surface tension anymore. Microfluidic chips can thus be fabricated in a material that is suited best for a particular assay while also being compatible with technical and economic requirements related to the production process. The fact that the flow in Eq. (1) can be reversed (pumping liquids back to the centre) in a controlled manner offers the advantage of managing efficiently the footprint of the device, providing the opportunity to integrate more functions in a compact format and leading ultimately to both miniaturization and a significant reduction in cost per assay.

The main advantage of the proposed approach hence relates to the fact that the complexity required by a specific protocol is moved from the microfluidic chip to the centrifugal platform itself. Instead of a simple spinning motor shaft driving a complex microfluidic chip, we propose a slightly more complex centrifugal platform with integrated pumps, electromechanical valves and electronic circuitry driving a simple and straightforward microfluidic chip. We believe that this approach is advantageous for any application where assays involving a large number of steps have to be performed with single-use microfluidic devices. Also, while the cost of the hardware required for this technology would obviously be higher compared to a basic centrifugal microfluidic setup, complex biological assays require centrifugal platforms with temperature control hardware, imaging system, detection equipment, control software, etc. Therefore, we believe that the additional complexity involved with the integration of valves and pumps would not necessarily be a limiting factor to the overall cost of the instrumentation.

3 Materials and methods

3.1 Instrumentation

The design of the active pneumatic centrifugal platform in Fig. 1b was optimized to ensure reliable operation of critical active components (i.e., pumps and electromechanical valves) despite the presence of a high centrifugal acceleration that can easily exceed $100g$, were $g = 9.8\ \mathrm{m/s^2}$ is the gravitational acceleration on Earth. The rotation of the platform was mediated by a stepper motor (T23NRLH-LDN-NS-00; Kollmorgen, Radford, VA) controlled by a stepper driver (P7000; Kollmorgen). The pneumatic connections to the microfluidic devices are made with a manifold placed 5 cm away from the centre of rotation. The platform is built to accommodate devices measuring up to 5 cm in width and 10 cm in length. A slip-ring with 10 independent electrical connections (EC3848; Moog, Inc., East Aurora, NY) was mounted on the motor shaft and used to power the platform during the rotation and transfer USB communications between the external computer and two on-board Arduino microcontrollers. One microcontroller was used for the electronic control of the 16 ultra-miniature latching solenoid valves (Series 120; The Lee Company, Westbrook, CT), the pump (P200-GAS-5V; Xavitech, Härnösand, Sweden) and the pressure sensor (HDIB001GUZ8H5; First Sensor, Inc., Mansfield, MA). The pneumatic connections of the 16 valves were made to create 8 independent pneumatic lines that can be switched between atmospheric pressure and the pressure provided

Lab on a Chip Accepted Manuscript

by the pump. The switching time of the valve is less than 1 ms, providing very accurate temporal control of the applied pressure. The microcontroller can also modify the speed of the pump to adjust the pressure between 0 to 5 psi above atmospheric pressure. The second microcontroller is used to control four 2×2 cm^2 thermoelectric elements and measure the temperature in real-time using four thermocouples. All active components were operational up to a rotation speed of about 1200 rpm, at which point the pump was found to slow down gradually. Although a platform operating at higher rotation speed could be easily designed (e.g., using an external pumping system combined with a pneumatic slip-ring), we have found that all fluidic functions required for developing bioanalytical assays could be performed reliably at rotation speeds of 1000 rpm or less using the electromechanical parts described herein.

Images of the device under rotation were obtained by using a digital camera (PL-A742; PixeLINK, Ottawa, ON) and a flash activated by a home-built triggering circuit sending a signal synchronized with the rotation of the platform. The high-speed movie shown in Movie_Fig5_2 of the Supplementary data was obtained by imaging the entire rotating platform with a fixed GigaView camera at 500 fps (HIS, Mississauga, ON). Software image processing was performed to remove the platform rotation and better visualize the fluid displacements in the microfluidic device. DNA content was determined through optical inspection using a NanoDrop UV/vis spectrophotometer (Wilmington, DE). Intrinsic signals from buffer solutions were used as a baseline for these measurements.

3.2 Chip fabrication

Microfluidic devices were fabricated in thermoplastic elastomers (TPE) using a process described in details elsewhere.[33] Mediprene OF 400M TPE was received in the form of pellets from Hexpol TPE (Elasto, Åmål, Sweden) and was extruded at 165 °C to form sheets of several meters in length and 3 mm in thickness. SU-8 moulds were prepared using standard photolithography. Epoxy moulds (epoxy resin: Conapoxy FR-1080; Cytec Industries, Woodland Park, NJ) were then replicated from the SU-8/silicon master mould using an intermediate replication process with poly(dimethylsiloxane) (PDMS, Sylgard 184; Dow Corning, Midland, MI). Hot-embossing of TPE was performed with an EVG 520 system (EV Group, Schärding, Austria) at a temperature of 120 °C, an applied force of 5 kN, and a pressure of 10^{-2} mbar. Access holes were punched in manual fashion followed by cutting the piece to its final dimensions (5×10 cm^2). The flat bottom layer (0.5 mm in thickness) was fabricated from Zeonor 1060R (Zeon Chemicals, Louisville, KY) using an Engel 150 injection moulding apparatus. Assembly and bonding of embossed TPE and flat Zeonor layers was performed by simply bringing the two parts in contact followed by annealing in an oven at 50 °C for 12 h to improve adhesion between the two layers. Fabrication steps were carried out in a clean room (class 1000) environment.

3.3 Reagents

Silica beads (with a nominal diameter of 20 µm) were purchased from Daiso Co., Ltd. (Osaka, Japan). Bead beds were formed from a suspension containing 30 mg/mL in 5% (v/v) glycerol/water. TE buffer (10 mM Tris, 1 mM EDTA, titrated to pH 7.6 using HCl) and guanidine hydrochloride (GuHCl) were both obtained from Sigma-Aldrich. Genomic DNA from *Salmonella enterica* subsp. *enterica* (*ex* Kauffmann and Edwards) Le Minor and Popoff serovar Paratyphi B (ATCC BAA-1250D-5) was acquired from American Type Culture Collection (Manassas, VA). The sample was dissolved in TE buffer containing 6 mM GuHCl to provide an initial concentration of 2.6 ng/µL.

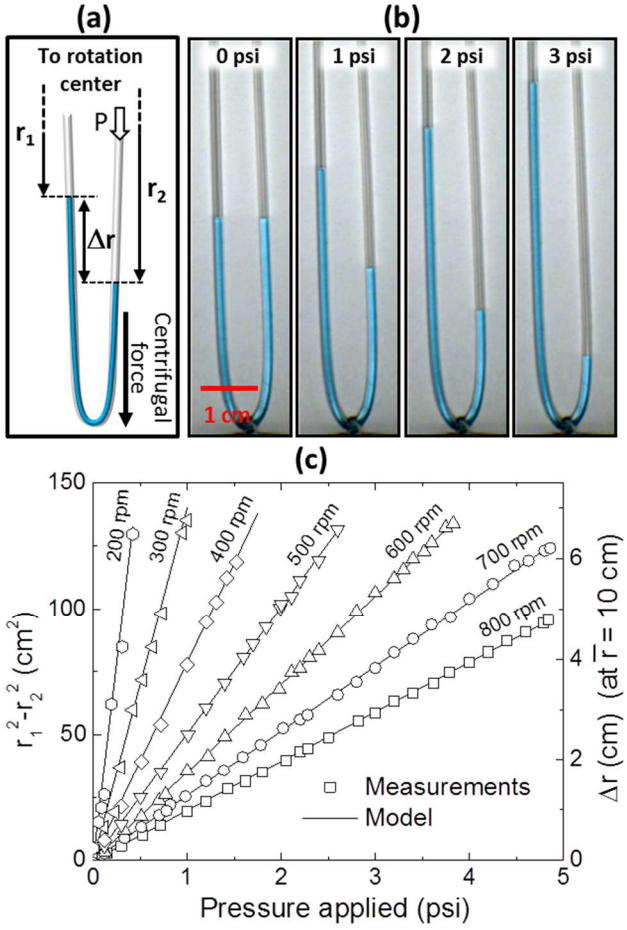

Fig. 2 Evaluation of the relation between the pressure difference applied and liquid rise on the centrifugal microfluidic platform. (a) Schematic of the U-shaped tubes used in the calibration experiment. (b) Images of the test structure partially filled with an aqueous solution of a blue-coloured dye. Pressure differences were applied through the pressure manifold as indicated at the top of these images (ω = 600 rpm and $\bar{r}$~10 cm). (c) Plot of liquid displacements (measured and predicted) at different rotation speeds and applied pressures. Experimental errors correspond to about ±0.05 psi for pressure and ±0.3 mm for position measurements.

4 Results and discussion

4.1 Control of fluid displacement

We first performed a series of simple experiments to demonstrate the level of control the platform provides for fluid displacement during rotation (Fig. 2). A U-shaped tube (internal diameter = 0.76 mm), partially filled with an aqueous solution, was placed

Lab on a Chip Accepted Manuscript

on the rotating platform and connected to the pressure manifold at one end while the other one was left open (Fig. 2a). As shown in Fig. 2b, the centrifugal force ensures that the liquid level is the same on both sides of the tube unless a pressure difference is applied, giving rise to liquid displacement and a new equilibrium position. Fig. 2c shows the effect of both the rotation speed and pressure applied on the liquid displacement. The results demonstrate that the liquid can be continuously and accurately displaced over a range of 0 to 7 cm using the 0 to 5 psi pressure range provided by the platform (for $(r_1 + r_2)/2 = \bar{r} \sim 10$ cm). Very good agreement is obtained with the theoretical prediction of Eq. (1) (Q = 0 in equilibrium), indicating that the pressure generated by the pump is well applied to the access ports with no significant losses through the pressure manifold.

It is important to note that, in microfluidic devices, capillary forces can also become significant because of the small dimension of the channels. Thus, at low rotation speeds, the additional presence of capillary action and contact angle friction forces can prevent the liquid from flowing according to Eq. (1) and reach the bottom of the reservoirs and channels. It then becomes difficult to create predictable liquid displacements using pneumatic pressure. In other words, it is only by combining the relatively high centrifugal force fields with controlled pneumatic pressure that the precise liquid displacements shown in Fig. 2c can be obtained in microfluidic devices. For example, for microfluidic devices containing channels with an effective hydraulic diameter of 100 μm or more, we have found that a rotation speed on the order of 400 rpm (at $\bar{r} \sim 10$ cm) is typically sufficient to minimize the effect of capillary forces and achieve accurate control over the liquid displacements. On the other hand, if smaller features (channels) are required in a specific application, we can always maintain an optimal rotation speed while increasing the pressure applied at designated ports to achieve necessary control and desired flow rate regime.

4.2 Valving

For many microfluidic applications, the flow of liquids on the chip has to be synchronized and one must be able to initiate and stop fluid motion on demand. In centrifugal microfluidics, this is usually done by the use of capillary[1, 15] and siphon[16] valves. Using active pneumatic pumping, the implementation of valving is similar to the siphon-based concept proposed by Siegrist *et al.*[16] in the sense that it uses a reservoir connected to a siphon channel to hold the liquid (Fig. 3a, stage 1). However, instead of using capillary force to prime the siphon and release the liquid from the reservoir, we couple the access port (vent) of the reservoir to the pressure manifold. By increasing the pressure at the access port ($p > p_{atm}$) the liquid is pushed away from the reservoir and advances toward the crest of the siphon (stage 2 of Fig. 3a). The minimal pressure required to reach the crest can be easily evaluated from Eq. (1). After the siphon crest is reached and the meniscus advances below the liquid level in the reservoir, the flow is primed (stage 3) and pressure at the port can thus be released without stopping the flow (i.e., the port is becoming equivalent to a regular vent V). It is noteworthy that the pressure could also be maintained if an increase in the liquid flow rate out of the reservoir is desired. Also, the same functionality can be achieved in a negative pressure regime (i.e., $p < p_{atm}$ using a vacuum pump). In this case, the outlet of the siphon channel is connected to an active access port that can aspirate air from the reservoir and trigger flow similarly to the positive pressure approach depicted in Fig. 3a.

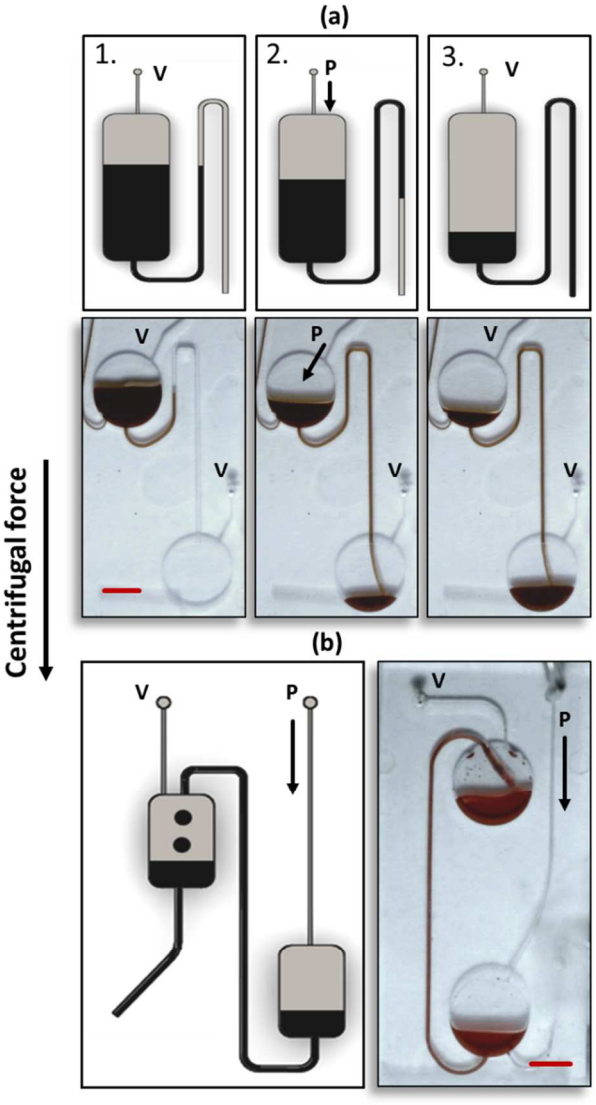

Fig. 3 Fluid displacement on a centrifugal chip using active pneumatic pumping. (a) Schematics (top panel) and sequential images (bottom panel) of a siphoned chamber that implements a valving function. Scale bar: 4 mm. (b) Schematic (left-hand side) and image (right-hand side) of a microfluidic assembly implementing reverse pumping. Scale bar: 4 mm. Accompanying materials showing complete mechanisms of active pneumatic valving and reverse pumping are available online as Supplementary data movie files Movie_Fig3a and Movie_Fig3b.

In the demonstration shown in Fig 3a, a pressure pulse of only 100 ms at 2 psi was found to be sufficient to prime reliably the siphon valve and initiate liquid flow out of the reservoir at ω = 600 rpm. At this rotation speed the dimensions of the siphon channel (300×300 μm^2) and the reservoir (800 μm deep) are large enough to prevent significant capillary effects from taking place

Lab on a Chip Accepted Manuscript

so that, in the absence of any applied pressure, centrifugal force ensures that the liquid level is the same in both reservoir and siphoning channel (stage 1 in Fig. 3a). This demonstrates that ultra-fast and on-demand priming of siphon valves can be achieved with the developed platform without the need to stop the rotation. Also, compared with the classical capillary[1, 15] and siphon[16] valves, multiple valves can be easily operated in an independent manner without undesirable interactions.

4.3 Reverse pumping

Pumping liquids back to the centre of rotation is of crucial importance in centrifugal microfluidics to overcome limitations related to the well-known "footprint" issue. In the proposed active pneumatic pumping approach, the solution to this problem is straightforward. As shown in Fig. 3b, pressure is applied at the access port of the bottom reservoir to push the liquid in the connecting channel up to the top reservoir. Contrary to the siphon valve of Fig. 3a, no liquid priming occurs in this configuration and the liquid left in the channel flows back to the bottom reservoir when the pressure is released. For an irreversible transfer between the two reservoirs, we can connect the transferring channel at the top of the destination reservoir (as illustrated in Fig. 3b). One has the possibility, however, to connect the channel at the bottom of the second reservoir and eventually use the centrifugal field to reverse the flow back from the second to the first reservoir. This application could be useful in assays where capture of target analyte by a functionalized surface is desired since the probability of capture is drastically increased by recirculating the sample back and forth several times.

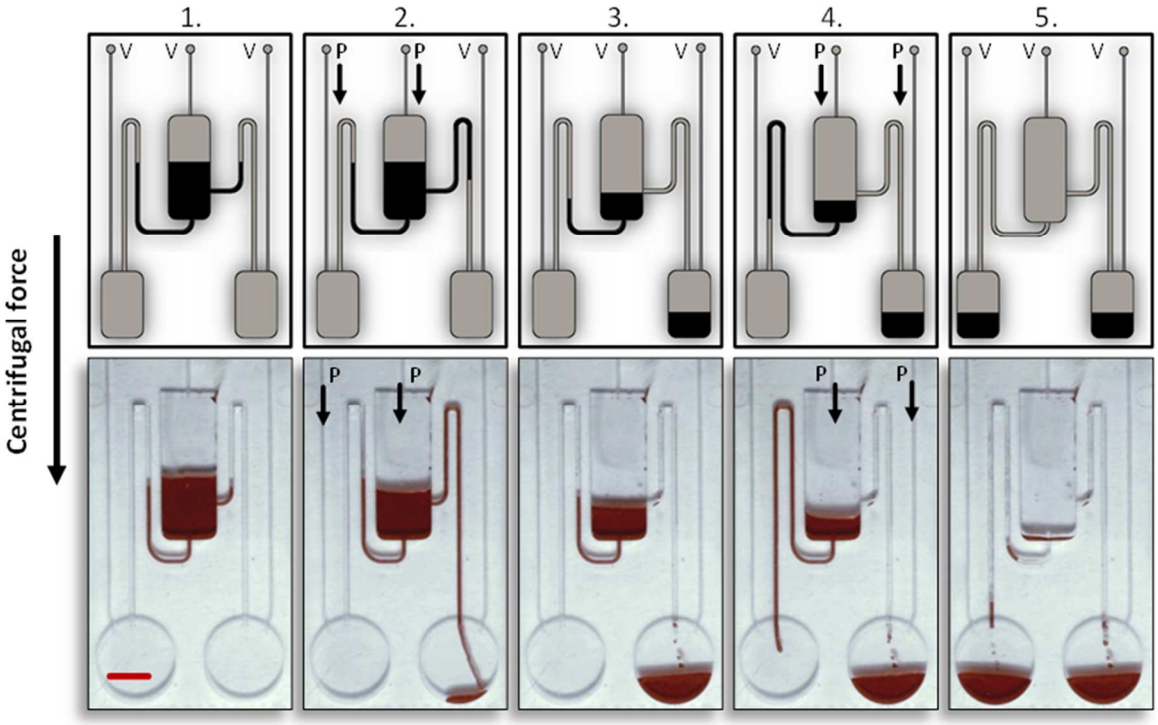

Fig. 4 Two-way switching based on active pneumatic pumping. Schematics (top panels) and sequential images (bottom panels) depict the process of distributing fluid over two downstream reservoirs. The scale bar corresponds to 4 mm. Supplementary material showing the complete mechanism of fluidic switch implemented by active pneumatic pumping approach is available as Supplementary data movie file Movie_Fig4.

In typical operation conditions (e.g., ω = 600 rpm and $\bar{r}$ ~10 cm), the pressure provided by the pump (up to 5 psi) was found to be sufficient to rapidly transfer the liquid to the top reservoir against the centrifugal force. Indeed, for the microfluidic devices shown in Fig. 3b, a single 100 ms pressure pulse at 2.0 psi leads to the transfer of about 8 μL from the bottom to the top reservoir (ω = 600 rpm), thus providing the possibility to transfer the entire 40 μL volume of the bottom reservoir in less than one second. The demonstration reveals superior efficiency of our system compared to the air jet approach,[25] where reverse pumping was not only slow (60 s for 68 μL) but also limited to very low rotation speeds (ω ~ 180 rpm).

4.4 Switching

A very difficult problem for centrifugal microfluidics is to switch liquid flows between two or more pathways in order to redirect them into different chambers. An example of such an operation can be encountered in assays where a captured specimen (e.g., DNA, protein or bacteria) has to be released in a clean buffer liquid after capture. An attempt in this direction has been made recently by using the Coriolis effect[34] but the physical size of the actual switching element and the rotational speeds required to achieve accurate control are not always practical. Asymmetric

Lab on a Chip Accepted Manuscript

capillary valves, named gate valves, have also been designed to enable switching of a liquid between two reservoirs depending on the rotation speed.[35] However, being based on capillary action, the proposed valves can suffer from the same drawbacks and limitations as standard capillary valves.

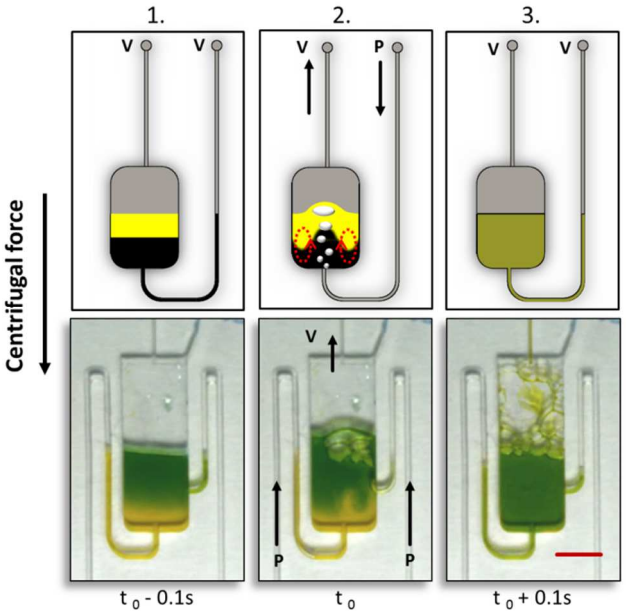

Fig. 5 Ultra-fast bubble-based mixing of liquid components in a microchamber. The schematics (top panels) and sequential images (bottom panels) illustrate the transformation of an unmixed sample containing two dyes into a homogeneous solution using air bubbles that are generated through active pneumatic pumping. Scale bar: 4 mm. Supplementary material showing the complete process of ultra-fast bubble-mixing implemented by active pneumatic pumping approach as well as the formation and dynamics of air bubbles at different rotation speeds is available as Supplementary data movie files Movie_Fig5_1 and Movie_Fig5_2, respectively.

In the active pneumatic pumping approach, liquid switching can be achieved by using the configuration shown in Fig. 4, where a central reservoir is coupled to two destination reservoirs through two siphon channels. The access ports of all reservoirs are connected to the pressure manifold. In the absence of any applied pressure, the liquid remains in the reservoir indefinitely during spinning (Fig. 4, stage 1). To transfer the first portion of liquid, pressure is applied simultaneously to both the central reservoir and the left-hand side reservoir. As a result, liquid moves along the right-hand side siphon channel until priming occurs and liquid is transferred into the respective downstream reservoir (stage 2). The process stops once the liquid level in the central reservoir has decreased below the connection point with the right-hand side siphon channel (stage 3). To transfer the liquid remaining in the central reservoir, pressure is now applied simultaneously to both the central reservoir and the right-hand side downstream reservoir. As a result, liquid flows into the left-hand side siphon channel that is connected on the bottom of the central reservoir (stage 4). In this example, the lowest connection point has been implemented at the bottom of the central reservoir, which allows the central chamber to be emptied completely (stage 5). The method thus provides a means of precisely metering the volumes of liquid to be split depending on the connection point of the siphon channels. For example, connecting the left-hand side siphon channel at a higher position to the central reservoir would allow for retaining some of the initial sample liquid in the central reservoir, which can be relevant for applications where only a certain amount of supernatant has to be extracted. The liquid switching experiment shown in Fig. 4 was performed using conditions similar to those of standard valving (i.e., 100 ms pressure pulse at 2 psi, see Fig. 3a and associated discussion) except that two pneumatic lines were pressurized simultaneously.

4.5 Mixing

Mixing is a long-standing issue in microfluidics due to low Reynolds numbers and associated laminar flow. We have found that the integration of active pneumatic pumping in centrifugal microfluidics offers a new and surprisingly efficient method to mix liquids inside microfluidic devices. We demonstrate this function using a reservoir that is connected to the manifold through a channel at the top and at the bottom, respectively (Fig. 5). The sample liquid initially consists of two distinct components (stage 1). Using the upper channel as a vent, it is possible to push air through the lower channel into the reservoir to create air bubbles that rise in the liquid (stage 2) against the centrifugal force field. The fluid convection currents associated with the rise of the air bubbles in the reservoir was found to mix very efficiently multiple liquid components (stage 3). In the experiment depicted in Fig. 5, a quick 100 ms pressure pulse of 1.5 psi was applied to the channels connected to the microfluidic reservoirs at a rotation speed of 600 rpm, which proved sufficient to obtain a well-mixed (homogeneous) solution. The high centrifugal force ensures that no liquid is pushed out of the device by the air bubbles. Note that, because the imaging system can only acquire one image per turn during the rotation of the platform (i.e., 10 images per second at 600 rpm), the temporal resolution of the image sequence is not high enough to capture all the details of the bubble creation and associated mixing. Additional detail is provided in Supplementary data file Movie_Fig5_2, where high-speed (500 fps) imaging of the bubble formation and displacement inside the microfluidic chamber is shown at rotation speeds of 600 and 1200 rpm is shown.

The sequential images shown in Fig. 5 demonstrate that on-demand ultra-fast mixing can be easily performed with short pressure pulses using the active pneumatic platform presented herein. This novel process appears to offer drastic improvement on the speed and efficiency of mixing compared to other approaches.[31, 36] The bubble-induced agitation can also be useful to reduce incubation time, resuspend particles, or even adjust the amount and type of gas dissolved in a liquid, which could be of key interest for the integration of various bioanalytical assays in microfluidics.

While a detailed analysis of the air bubble mixing process is beyond the scope of the present paper, it is interesting to review the conditions necessary to create bubble mixing in microfluidics. Briefly, the acceleration and associated buoyancy forces should be strong enough to displace the air bubbles upward before their size becomes large enough to drag liquid out of the device. For a given geometry, the size at which a bubble detaches from a

Lab on a Chip Accepted Manuscript

surface and rises depends on the relative importance of buoyancy and surface tension.[37] The Bond number (Bo), which represents the relative importance of buoyancy and surface tension, is thus of interest to evaluate if bubble-mixing is possible:

$$\mathrm{Bo} = \frac{\Delta\rho a_{cp} L^2}{\gamma} \quad (2)$$

where $\Delta\rho$ is the liquid-air density difference, a_{cp} is the centripetal acceleration, L is a characteristic length (diameter of the air bubble, for example) and γ the surface tension. In standard microfluidics, bubble mixing is not possible because gravitational force alone is too low to displace air bubbles before they become larger than the microfluidic chamber (e.g., using $a_{cp} = g, \gamma = 0.072$ N/m, $\Delta\rho = 1000$ kg/m^3 and $L = 500$ µm, Bo $\approx 0.034 \ll 1$). By increasing the centripetal acceleration to $a_{cp} = 40g$, as is the case for our experiment in Fig. 5, the Bond number becomes Bo ≈ 1.4, thus indicating that buoyant forces become significant. Also, we have observed experimentally that the size of the air bubbles created in the microfluidic reservoir decreases as a function of the rotation speed (see Supplementary data file Movie_Fig5_2), thus confirming a predominant role of the centrifugal acceleration on the air bubble dimensions. It is thus only by combining the high acceleration provided by the centrifugal microfluidic platform (to increase the Bond number) and the active pneumatic pumping (to pump air against a strong centrifugal field) that the bubble-based mixing becomes possible in microfluidics. Further work is ongoing to characterize and model this novel mixing process in more detail.

4.6 Application to a bioanalytical assay: DNA extraction

To demonstrate the potential of the developed active pneumatic centrifugal platform to integrate a complete bioanalytical assay, we designed a microfluidic cartridge to perform solid-phase extraction (SPE) of DNA in an automated fashion. SPE is a standard method for separating nucleic acids from cellular components that interfere with downstream analysis based on PCR or sequencing techniques. Silica is widely used as an extraction matrix in commercial DNA purification kits and has also been employed for extraction of nucleic acids on microchips.[38-40] Such devices typically have used silica particles packed inside a designated column (or extraction chamber). The use of microfabricated silica pillars produced by reactive ion etching has also been reported.[41] Adsorption of DNA becomes possible by reducing both the negative charge of the silica surface and the affinity of surrounding water molecules through the use of buffer solution with a high ionic strength.[38] An alternative mechanism involves GuHCl as a chaotropic agent that denaturates nucleic acids allowing positively charged ions to form a salt bridge between the DNA phosphate backbone and the silica surface (being both negatively charged) at high ion concentration.[39] Contaminants are removed from the extraction matrix in a rinse step. DNA is finally released from the surface by introducing water or elution buffer to the column. Herein, we demonstrate extraction of genomic DNA from *S. enterica* mediated by GuHCl in TE buffer using a bead bed composed of monodispersed silica particles (20 µm in diameter) as an extraction matrix. The sample solution comprises 300 µL and contains DNA at a concentration of $c_0 = 2.6$ ng/µL. After passage of the sample, the bead bed is washed with 50 µL of 95% isopropanol. DNA is eluted at 60 °C using 30 µL of TE buffer (corresponding to one tenth of the initial sample volume).

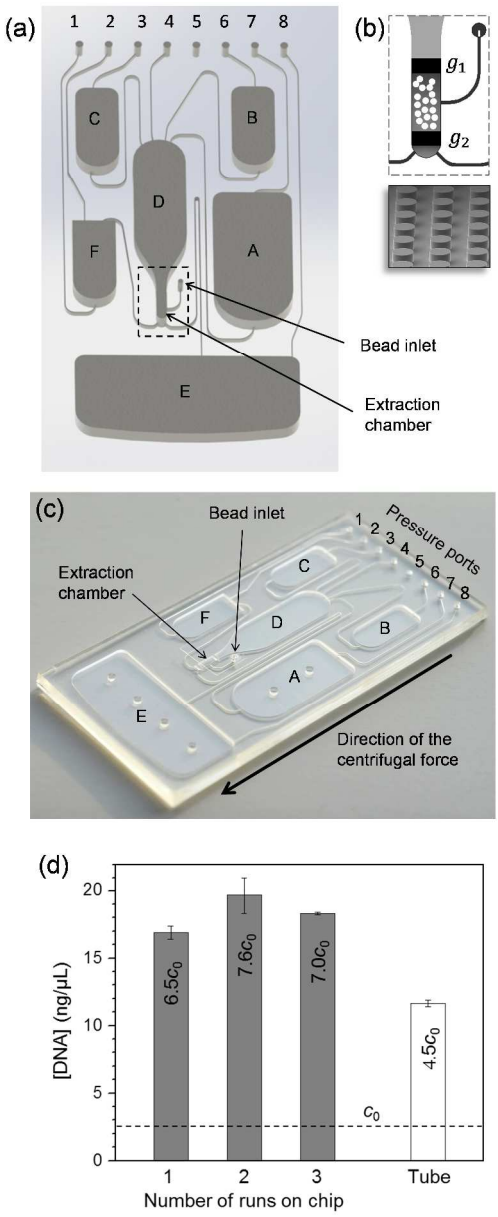

Fig. 6 DNA extraction using silica particles on a centrifugal microfluidic chip. (a) Schematic design of the microfluidic chip illustrating arrangement of reservoirs, connecting ports and communication channels. (b) Zoom of the region delimited by the dotted rectangle depicting the working principle of using two gate structures to confine beads within the extraction chamber. The scanning electron micrograph shows the pillar array that was implemented in the two gate structures (g_1 and g_2). The pillars in this image have a diameter of 20 μm. (c) Photograph of the 5×10 cm^2 cartridge. (d) Plot of measured DNA content and concentration factors for three runs conducted with genomic DNA from *S. enterica* using the same extraction column. The dashed line denotes the initial sample concentration c_0. The outcome of a control experiment performed in an Eppendorf tube has been included for comparison. Concentration factors have been calculated using a nominal volume of 30 µL for the elution buffer. Error bars represent standard deviations obtained from three optical measurements. Supplementary material showing the microfluidic flow in this experiment is available as Supplementary data movie file Movie_Fig6.

Lab on a Chip Accepted Manuscript

Microfluidic features and their arrangement on the cartridge are depicted in Fig. 6a. The chip does not contain any active elements, required no specific surface treatments and was fabricated simply by embossing a TPE layer, punching access holes and bonding to a Zeonor slide (see Section 3.2 for details). Pressure access ports are used to load reagents to their designated reservoirs using a micropipette. Reservoir A (connected to port #7) contains the DNA sample solution, B (connected to port #6) the isopropanol, and C (connected to port #3) the elution buffer. The central unit D (connected to port #4) serves as a transfer reservoir and incorporates the extraction chamber. Beads are inserted through a separate entry which is sealed afterwards using a polymer fibre. Upper and lower ends of the extraction chamber are gated with a pillar array to confine the beads within the cavity as illustrated in Fig. 6b. The waste reservoir E (connected to port #8) is used to collect sample solution and isopropanol after passing through the bead bed. Reservoir F, which initially remains empty, is designated to accommodate the eluted DNA sample at the end of the process. All components are loaded onto the cartridge before it is mounted on the centrifugal platform. An actual photograph of the fabricated and assembled chip before use is shown in Fig. 6c.

The detailed fluidic protocol used in this assay can be visualized in Supplementary data movie file Movie_Fig6. The process begins with spinning at 600 rpm (with no additional pressure applied) to displace liquids at the bottom of each reservoir. Sample liquid is transferred in 50 μL aliquots from A to D by applying a pressure of 3 psi to port #7. Passage of liquid across the bead bed is then mediated by activating ports #1 to #7 simultaneously. When leaving the extraction chamber, sample is transferred into the waste through the siphon linking reservoirs D and E. The process is repeated until the entire sample volume has passed through the bead bed. Between each step, we maintained a small portion of liquid (e.g., 5 µL) in reservoir D to prevent the bead bed from drying. When completed, port #6 is activated to transfer 50 µL of isopropanol from B to D. The rinse step proceeds by activating ports #1 to #7 until all liquid is flushed into E. Then port #3 is activated to relocate the elution buffer from C to D which is followed by heating the extraction chamber to 60 °C for 2 min using one of the thermoelectric elements of the platform. Elution buffer is slowly passed across the bead bed over a period of about 2 min and collected in reservoir F by activating ports #3 to #8. At the end of the process, the heater is switched off and pressure is released before the centrifugal system is brought to a standstill. The eluted sample is recovered from the chip through port #1 using a micropipette. From a fluid manipulation perspective, it is interesting to note that the assay could be completed successfully despite the very large variability in the wetting properties of the various buffers (i.e., isopropanol wets the chip surfaces while aqueous solutions do not), which would have been challenging to achieve in classical centrifugal microfluidics using standard siphon or capillary valves.

The findings presented in Fig. 6d confirm the possibility of isolating genomic DNA with relatively high yield in a fairly reproducible manner. In this example, we performed three subsequent extraction experiments with the same chip (while the bead bed has been rinsed thoroughly between each run to limit possible effects from accumulation of left-over DNA). We found concentrations of eluted DNA to be between 16.9 and 19.7 ng/µL, which accounts for concentration factors of 6.5 to 7.6c_0. We estimate that capture efficiencies as high as 80% are achievable when taking into account that residual wash solution remaining in the bead bed can increase the volume of the elution buffer by 10% or more (data not shown). Yields were lower (e.g., 11.7 ng/µL; 4.5c_0) when we performed SPE in a standard Eppendorf tube. In this control experiment, DNA was extracted from 300 µL sample using 3×100 µL aliquots that were agitated with silica particles over a total of 20 min. Beads were rinsed two times with 25 µL of 95% isopropanol before eluting DNA in 30 µL TE buffer at 60 °C for 5 min. After each step, the tube was centrifuged to sediment the silica particles before removal of the supernatant. The findings confirm that interactions between DNA molecules and free-floating silica particles are less efficient compared to funnelling sample solution through a narrow, well-packed column on the chip. Previous studies, nevertheless, have shown relatively high variability in capture efficiencies for DNA extraction using silica particles on microchips.[38] Variation in the number of beads and their packing density can largely affect performance of the extraction process. We believe that the centrifugal system presented herein is likely to benefit the formation of densely-packed bead beds while reducing batch-to-batch variability. The use of monodispersed silica particles seemed equally important to the formation of extraction columns that can be reused several times while preserving their integrity to a large extent.

5 Conclusion

We have shown that the unique combination of centrifugation and active pneumatic pumping provides an effective means of precisely controlling liquid displacements and generating robust and efficient fluidic functions such as valving, switching and reverse pumping using simple microfluidic devices. The platform thus offers the interesting prospect of overcoming traditional problems related to capillarity and limited footprint, which in turn broadens the scope of possible applications that become feasible using centrifugal microfluidics. Moreover, we have found that decoupling the design of the microfluidic chips from the wetting properties of the supporting materials allows for better control and higher reproducibility of fluidic processes while simplifying drastically the microfluidic design. The platform also offers the possibility of performing bubble-based mixing, which provides a simple and effective solution to a long standing issue in microfluidics. Finally, we have demonstrated the integration of a complete DNA harvesting assay, suggesting that complex biological and analytical protocols may be integrated without imposing constraints on footprint and performance of the device.

Future work will focus on improving the hardware platform to enable higher rotation speeds and increase the number of microfluidic tests that can be performed simultaneously. Indeed, while all the fluidic operations required for complex protocols could be performed reliably under 1000 rpm, limitations in the maximum rotation speed can affect the range of applications where high centrifugal force fields are necessary (such as blood fractionation, bacteria concentration, etc.). Also, while the developed platform can control two microfluidic devices, we have found that multiplexing the number of tests may present

Lab on a Chip Accepted Manuscript

additional challenges compared to classical microfluidics (achieve reliable pneumatic connections to multiple microfluidic devices simultaneously, etc.).

Finally, the integration of active pneumatic pumping in centrifugal microfluidics also offers a number of other interesting applications that have not been covered in this work. For example, the possibility of modulating the applied pressure by controlling the hydraulic resistance of the air channels and inducing dynamic and retarding effects could be used to create permanently circulating flows that are difficult to implement in traditional centrifugal microfluidics. The principle of circulating air within the system may further be extended to applications that require the presence of gaseous components in both on-chip and off-chip reservoirs. Combined with thermal control and electromagnetic actuation, the platform proposed herein offers all the elements required to perform complete sample-to-answer assays where lysis, PCR as well as various detection techniques may all be integrated in a technologically convenient manner.

Acknowledgement

This work was supported in part by the GRDI-funded program "Strengthening Food and Water Safety in Canada through an Integrated Federal Genomics Initiative". We thank François Normandin for his technical work on the platform design, electronic circuits and control software as well as our colleagues Harold Hébert, Maxence Mounier, Hélène Roberge, Jamal Daoud and Alex Boutin for technical assistance and useful discussions.

Notes and references

[a]*National Research Council of Canada, 75 de Mortagne, Boucherville, Quebec, Canada, J4B 6Y4. Fax: 1 450 641-5105; Tel: 1 450 641-5232; E-mail: Teodor.Veres@cnrc-nrc.gc.ca*

‡ These authors contributed equally to the work.

1. J. Ducrée, S. Haeberle, S. Lutz, S. Pausch, F. von Stetten and R. Zengerle, *J. Micromech. Microeng.*, 2007, **17**, S103-S115.
2. G. Jia, K. S. Ma, J. Kim, J. V. Zoval, M. J. Madou, S. K. Deo, S. Daunert, R. Peytavi and M. G. Bergeron, *Proceedings of the SPIE International Symposium-Photonics Europe*, Strasbourg, 2004.
3. J. V. Zoval and M. J. Madou, *Proc. IEEE*, 2004, **92**, 140-153.
4. M. Czugala, D. Maher, F. Collins, R. Burger, F. Hopfgartner, Y. Yang, J. Zhaou, J. Ducrée, A. Smeaton, K. J. Fraser, F. Benito-Lopez and D. Diamond, *RSC Adv.*, 2013, **3**, 15928-15928.
5. R. Gorkin, J. Park, J. Siegrist, M. Amasia, B. S. Seok Lee, J.-M. Park, J. Kim, H. Kim, M. Madou and Y.-K. Cho, *Lab Chip*, 2010, **10**, 1758-1773.
6. H. Chen, X. Li, L. Wang and P. C. H. Li, *Talanta*, 2010, **81**, 1203-1208.
7. A. Date, P. Pasini and S. Daunert, *Anal. Chem.*, 2010, 349-356.
8. H. Kido, M. Micic, D. Smith, J. Zoval, J. Norton and M. Madou, *Colloid. Surf. B*, 2007, **58**, 44-51.
9. J. Kim, S. H. Jang, G. Jia, J. V. Zoval, N. A. Da Silva and M. J. Madou, *Lab Chip*, 2004, **4**, 516-522.
10. M. Focke, F. Stumpf, B. Faltin, P. Reith, D. Bamarni, S. Wadle, C. Müller, H. Reinecke, J. Schrenzel, P. Francois, D. Mark, G. Roth, R. Zengerle and F. von Stetten, *Lab Chip*, 2010, **10**, 2519-2526.
11. S. O. Sundberg, C. T. Wittwer, C. Gao and B. K. Gale, *Anal. Chem.*, 2010, **82**, 1546-1550.
12. H. Chen, L. Wang and P. C. H. Li, *Lab Chip*, 2008, **8**, 826-829.
13. R. R. Peytavi, F. R. Raymond, D. Gagné, F. J. Picard, G. Jia, J. Zoval, M. Madou, K. Boissinot, M. Boissinot, L. Bissonnette, M. Ouellette and M. G. Bergeron, *Clin. Chem.*, 2005, **51**, 1836-1844.
14. J. Melin, H. Johansson, O. Söderberg, F. Nikolajeff, U. Landegren, M. Nilsson and J. Jarvius, *Anal. Chem.*, 2005, **77**, 7122-7130.
15. M. Madou, J. Zoval, G. Jia, H. Kido, J. Kim and N. Kim, *Annu. Rev. Biomed. Eng.*, 2006, **8**, 601-628.
16. J. Siegrist, R. Gorkin, L. Clime, E. Roy, R. Peytavi, H. Kido, M. Bergeron, T. Veres and M. Madou, *Microfluid. Nanofluid.*, 2010, **9**, 55-63.
17. C. Lu, Y. J. Juang, C. G. Koh and L. J. Lee, *Annual Technical Conference ANTEC*, Charlotte, NC, 2006, **5**, 2566-2570.
18. V. Jokinen and S. Franssila, *Microfluid. Nanofluid.*, 2008, **5**, 443-448.
19. L. X. Kong, K. Parate, K. Abi-Samra and M. Madou, *Microfluid. Nanofluid.*, DOI 10.1007/s10404-014-1492-x.
20. J.-M. Park, Y.-K. Cho, B.-S. Lee, J.-G. Lee and C. Ko, *Lab Chip*, 2007, **7**, 557-564.
21. R. Gorkin, C. E. Nwankire, J. Gaughran, X. Zhang, G. G. Donohoe, M. Rook, R. O'Kennedy and J. Ducrée, *Lab Chip*, 2012, **12**, 2894-2902.
22. D. J. Kinahan, S. M. Kearney, N. Dimov, M. T. Glynn and J. Ducrée, *Lab Chip*, 2014, **14**, 2249-2258.
23. Z. Cai, J. Xiang, B. Zhang and W. Wang, *Sens. Actuat. B*, 2015, **206**, 22-29.
24. R. Gorkin, L. Clime, M. Madou and H. Kido, *Microfluid. Nanofluid.*, 2010, **9**, 541-549.
25. D. Mark, T. Metz, S. Haeberle, S. Lutz, J. Ducrée, R. Zengerle and F. von Stetten, *Lab Chip*, 2009, **9**, 3599-3603.
26. T. H. G. Thio, F. Ibrahim, W. Al-Faqheri, J. Moebius, N. S. Khalid, N. Soin, M. K. B. A. Kahar and M. Madou, *Lab Chip*, 2013, **13**, 3199-3209.
27. M. M. Aeinehvand, F. Ibrahim, S. W. Harun, W. Al-Faqheri, T. H. G. Thio, A. Kazemzadeh and M. Madou, *Lab Chip*, 2014, **14**, 988-997.
28. K. Abi-Samra, L. Clime, L. Kong, R. Gorkin, T.-H. Kim, Y.-K. Cho and M. Madou, *Microfluid. Nanofluid.*, 2011, **11**, 643-652.
29. M. C. R. Kong and E. D. Salin, *Anal.Chem.*, 2010, **82**, 8039-8041.
30. M. C. R. Kong and E. D. Salin, *Anal. Chem.*, 2011, **83**, 9186-9190.
31. M. C. R. Kong and E. D. Salin, *Microflud. Nanofluid.*, 2012, **13**, 519-525.
32. S. Haeberle, N. Schmitt, R. Zengerle and J. Ducrée, *Sens. Actuat. A*, 2007, **135**, 28-33.
33. M. Geissler, K. Li, X. Zhang, L. Clime, G. P. Robideau, G. J. Bilodeau and T. Veres, *Lab Chip*, 2014, **14**, 3750-3761.

Lab on a Chip Accepted Manuscript

34. J. Kim, H. Kido, R. H. Rangel and M. J. Madou, *Sens. Actuat. B*, 2008, **128**, 613-621.
35. A. Kazemzadeh, P. Ganesan, F. Ibrahim, M. M. Aeinehvand, L. Kulinsky and M. J. Madou, *Sens. Actuat. B*, 2014, **204**, 149-158.
36. J. Steigert, M. Grumann, T. Brenner, K. Mittenbühler, T. Nann, J. Rühe, I. Moser, S. Haeberle, L. Riegger, J. Riegler, W. Bessler, R. Zengerle and J. Ducrée, *J. Assoc. Lab. Autom.*, 2005, **10**, 331-341.
37. A. A. Kulkarni and J. B. Joshi, *Ind. Eng. Chem. Res.*, 2005, **44**, 5873-5931.
38. M. C. Breadmore, K. A. Wolfe, I. G. Arcibal, W. K. Leung, D. Dickson, B. C. Giordano, M. E. Power, J. P. Ferrance, S. H. Feldman, P. M. Norris and J. P. Landers, *Anal. Chem.*, 2003, **75**, 1880-1886.
39. H. Tian, F. R. Hühmer and J. P. Landers, *Anal. Biochem.*, 2000, **283**, 175-191.
40. K. A. Wolfe, M. C. Breadmore, J. P. Ferrance, M. E. Power, J. F. Conroy, P. M. Norris and J. P. Landers, *Electrophoresis*, 2002, **23**, 727-733.
41. N. C. Cady, S. Stelick and C. A. Bett, *Bionsens. Bioelectron.*, 2003, **19**, 59-66.

Lab on a Chip Accepted Manuscript